Near-Threshold Production of the Multistrange Ξ^- Hyperon

P. Chung,[1] N. N. Ajitanand,[1] J. M. Alexander,[1] M. Anderson,[5] D. Best,[4] F. P. Brady,[5] T. Case,[4] W. Caskey,[5] D. Cebra,[5] J. L. Chance,[5] B. Cole,[10] K. Crowe,[4] A. C. Das,[2] J. E. Draper,[5] M. L. Gilkes,[1] S. Gushue,[1,8] M. Heffner,[5] A. S. Hirsch,[6] E. L. Hjort,[6] W. Holzmann,[1] L. Huo,[12] M. Issah,[1] M. Justice,[3] M. Kaplan,[7] D. Keane,[3] J. C. Kintner,[11] J. Klay,[5] D. Krofcheck,[9] R. A. Lacey,[1] J. Lauret,[1] M. A. Lisa,[2] H. Liu,[3] Y. M. Liu,[12] J. Milan,[1] R. McGrath,[1] Z. Milosevich,[7] G. Odyniec,[4] D. L. Olson,[4] S. Panitkin,[3] N. T. Porile,[6] G. Rai,[4] H. G. Ritter,[4] J. L. Romero,[5] R. Scharenberg,[6] B. Srivastava,[6] N. T. B Stone,[4] T. J. M. Symons,[4] A. Taranenko,[1] J. Whitfield,[7] T. Wienold,[4] R. Witt,[3] L. Wood,[5] and W. N. Zhang[12]

(E895 Collaboration)

[1]*Departments of Chemistry and Physics, SUNY at Stony Brook, New York 11794-3400, USA*
[2]*The Ohio State University, Columbus, Ohio 43210, USA*
[3]*Kent State University, Kent, Ohio 44242, USA*
[4]*Lawrence Berkeley National Laboratory, Berkeley, California, 94720, USA*
[5]*University of California, Davis, California, 95616, USA*
[6]*Purdue University, West Lafayette, Indiana, 47907-1396, USA*
[7]*Carnegie Mellon University, Pittsburgh, Pennsylvania 15213, USA*
[8]*Brookhaven National Laboratory, Upton, New York 11973, USA*
[9]*University of Auckland, Auckland, New Zealand*
[10]*Columbia University, New York, New York 10027, USA*
[11]*St. Mary's College, Moraga, California 94575, USA*
[12]*Harbin Institute of Technology, Harbin, 150001 People's Republic of China*

H. Oeschler

Departments of Chemistry and Physics, SUNY at Stony Brook, New York 11794-3400, USA
and Darmstadt University of Technology, 64289 Darmstadt, Germany

(Received 18 February 2003; published 14 November 2003)

The yield for the multistrange Ξ^- hyperon has been measured in 6A GeV Au + Au collisions via reconstruction of its decay products π^- and Λ, the latter also being reconstructed from its daughter tracks of π^- and p. The measurement is rather close to the threshold for Ξ^- production and therefore provides an important test of model predictions. The measured yield for Ξ^- and Λ are compared for several centralities. In central collisions the Ξ^- yield is found to be in excellent agreement with statistical and transport model predictions, suggesting that multistrange hadron production approaches chemical equilibrium in high baryon density nuclear matter.

DOI: 10.1103/PhysRevLett.91.202301 PACS numbers: 25.75.Dw

Many years ago, it was proposed that strange particle yields could serve as an indicator for the formation of the quark-gluon plasma (QGP) [1]. For a partonic system with partially restored chiral symmetry, strangeness is expected to be readily produced due to the lower energy threshold for $s\bar{s}$ quark pair production. The production of strangeness may be further increased for significant baryon densities where the chemical potential associated with the production of light quarks is raised. For these reasons it is expected that the QGP phase should reflect a high strange (anti)quark density [2]. Because of their strange quark content, multistrange baryons (and antibaryons) are expected to be a more sensitive probe of this phase than hadrons which contain only one strange valence quark.

Interest in strangeness and especially in the yield of multistrange hadrons has grown enormously [3]. The observation of "strangeness enhancement" in the production of Ξ^- (dss) and Ω^- (sss) in heavy ion collisions compared to pp or pA collisions has contributed to the excitement [4].

A comparison of experimental and calculated yields indicates two distinct features: (i) Statistical models, with input of temperature and chemical potential, are in fair or good agreement with the yields reported from the BNL Alternating Gradient Synchrotron (AGS) [5], the CERN Super Proton Synchrotron (SPS) [6], and from recent experiments performed at the BNL Relativistic Heavy Ion Collider (RHIC) [7,8]. Using a canonical description this approach is successful even for beam energies of $\sim$1A GeV [9]. They can even explain the observed enhancement between pA and Pb + Pb collisions [10]. (ii) Transport model calculations based on hadronic interactions are currently unable to account for the measured yields of multistrange particles at SPS energies (158A GeV) [11]. The success of the statistical model is surprising and raises the question as to whether or not this success holds true for near-threshold multistrange particle production.

This Letter reports on the production of the singly strange Λ hyperon and the doubly strange Ξ^- hyperon in 6A GeV Au + Au collisions. Preliminary reports on Λ hyperon production have been given elsewhere [12]. The Ξ^- measurement reported here is unique in that it represents the lowest incident energy for which such a measurement has been made in heavy ion collisions (the laboratory energy threshold for direct production in NN collisions is 3.74 GeV). The production of multistrange hadrons is arguably most interesting close to the production threshold due to the suppression of multistep processes (the Ξ^- particle is mainly produced from the strangeness-exchange reactions $[\bar{K}(\Lambda, \Sigma) \rightarrow \Xi(\pi, \eta)]$. Collisions of 6$A$ GeV Au + Au are expected to produce nuclear matter with high baryon density and relatively low chemical freeze-out temperature. Thus, marked changes in the model predictions are expected for multistrange particle yields.

The experiment has been performed with the equation of state time projection chamber (TPC) [13] at the Alternating Gradient Synchrotron. Details on the detector and its setup have been reported earlier [12–14]. The data presented here benefit from the excellent coverage, continuous 3D tracking, and particle identification capabilities of the TPC. These features are crucial for the efficient detection and reconstruction of Λ's and Ξ^-.

Several studies have demonstrated the viability of vertex and trajectory reconstruction for V^0's, i.e., from a track pair resulting from two charged daughter particles [12,15,16]. However, a signature for the doubly strange Ξ^- must be demonstrated by finding the two consecutive decays: $\Xi^- \rightarrow \Lambda\pi^-$ followed by $\Lambda \rightarrow p\pi^-$. This requires locating three correlated tracks and is considerably more difficult, especially for low yields near the threshold. The upper and lower panels of Fig. 1 show signature peaks in the invariant mass spectra for primary Λ's and for the Ξ^-, respectively. The Ξ^- mass peak is well centered at its rest mass of 1.32 GeV. The width of the distribution for Ξ^- (FWHM) is 10 MeV compared to 6 MeV for the width of the Λ as can be expected from the resolution of the TPC.

A description for the reconstruction of primary Λ's is given in Refs. [12,15]. Ξ^- reconstruction proceeded via a combination of two distinct steps. In the first, primary and secondary Λ hyperons were reconstructed from the daughters of their charged particle decay, $\Lambda \rightarrow p + \pi^-$ (branching ratio $\sim$64%) following essentially the procedure outlined in Refs. [12,15], except that the training (see below) was different for Λ's that do not originate directly from the primary vertex (secondary Λ's). All TPC tracks in an event were reconstructed followed by

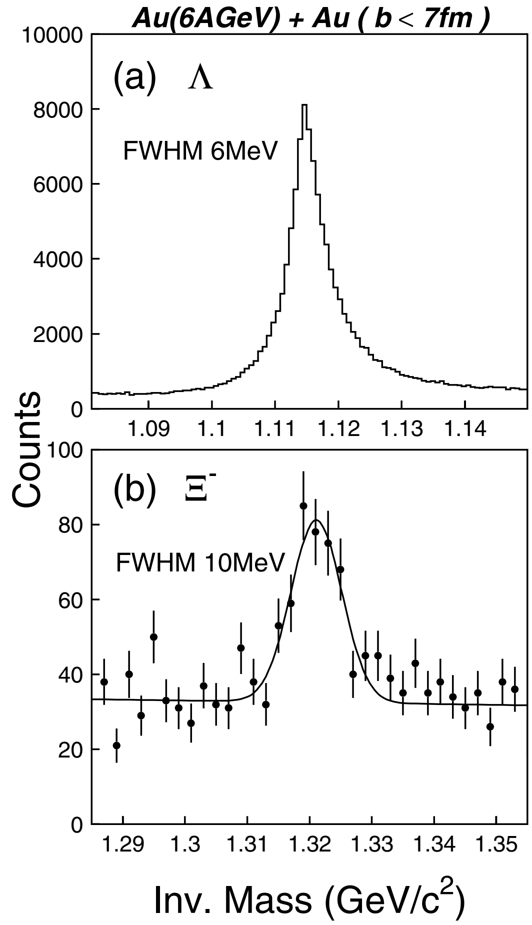

FIG. 1. Invariant mass spectrum for (a) Λ and (b) Ξ^- in 6A GeV semicentral Au + Au collisions ($b < 7$ fm). The curve in (b) is a Gaussian fit to the data points. The full widths at half maximum for the peaks are indicated. With these cuts there are $\sim$250 Ξ^- counts (net of background).

the calculation of an overall event vertex. Thereafter, each $p\pi^-$ pair was considered and their point of closest approach obtained. Pairs whose member trajectories intersect (with fairly loose criteria such as decay distance from the event vertex $>$0.5 cm) at a point other than the main event vertex were assigned as Λ candidates (primary and secondary) and evaluated to yield an invariant mass and associated momentum. These Λ candidates were then passed to a fully connected feed-forward multilayered neural network [16] trained to separate "true" secondary Λ's from the combinatoric background. The network was trained from a set consisting of true secondary Λ's and a set consisting of a combinatoric background. True secondary Λ's were generated by tagging and embedding simulated Λ's (created from the decay of Ξ^- particles from relativistic quantum molecular dynamics (RQMD) [17] calculations) in raw data events in a detailed GEANT simulation of the TPC. The combinatoric background or "fake" Λ's were generated via a mixed event procedure in which the daughter particles of the Λ ($p\pi^-$) were chosen from different data events.

In step 2, the Ξ^- particle was reconstructed from its weak decay: $\Xi^- \rightarrow \Lambda\pi^-$ (branching ratio = 100%; $c\tau$ = 4.9 cm), using the secondary Λ's found in step 1. To do this, each $\Lambda\pi^-$ pair was evaluated to assign Ξ^- candidates (and their associated invariant mass and momentum) which were passed to a fully connected feed-forward multilayered neural network [16] trained to separate true Ξ^-'s from the combinatoric background. For this latter step, the network was trained from a set consisting of true Ξ^-'s and a set consisting of a combinatoric background following a procedure similar to that described earlier for Λ's.

For the four centrality selections (central to peripheral) presented here, 71 656, 140 706, 154 542, and 57 236 events were processed to yield 78, 118, 100, and 16 Ξ^-'s, respectively. The corresponding number of primary Λ's are 21 526, 37 090, 30 973, and 6994, respectively. Relatively good phase space coverage was achieved for both the Ξ^-'s ($0 < p_T < 1.2$ GeV/c, $-0.5 < y_n < 0.5$) and the Λ's ($0 < p_T < 1.2$ GeV/c, $-0.7 < y_n < 0.6$). Here, y_n is the normalized rapidity. The detection efficiency for Ξ^- ranged from $5.4 \pm 0.4 \times 10^{-3}$ to $23.5 \pm 0.5 \times 10^{-3}$. Similar efficiencies for primary Λ's ranged from $2.3 \pm 0.2 \times 10^{-2}$ to $6.8 \pm 0.2 \times 10^{-2}$.

The neural network optimizes (during training) and then applies (during reconstruction) a multidimensional cut on topological variables or input neurons [16], to distinguish true Ξ^-'s. In addition, several "hard cuts" (e.g., $dca_{\Lambda,\pi}$, where dca is the distance of closest approach of a Λ, π to the event vertex) were employed to investigate and minimize systematic uncertainties. Figure 1 shows the results obtained with such restrictions. In general, tighter hard cuts led to improvements in the signal-to-background ratio, but with significant reductions in the raw yield due to poorer detection efficiencies. Nevertheless, the efficiency corrected yields showed essentially no dependence on these cuts.

For the different cut conditions there are, of course, different efficiencies for track finding and thus for Ξ^- and Λ reconstruction. These efficiencies have been determined by simulations that involve embedding Ξ^- particles from RQMD calculations into events from the data sample and running this modified data set through the neural network. Subsequently, the ratio of reconstructed Ξ^- particles in the real data divided by the simulated efficiency has been studied for a large variety of cut conditions. This method allows us to minimize systematic errors for the applied hard cut and thus we expect that statistical errors predominate. As a further test of this efficiency determination method, a model-independent integration over p_T and rapidity was made for Λ's. The result was in very good agreement with the method used here for both Λ's and Ξ^-'s.

Several centrality cuts have been made in order to examine the variation of the Ξ^- multiplicity on impact parameter and the number of participating nucleons A_{part}. For each centrality cut, an impact parameter range was assigned via its respective fraction of the minimum bias cross section as described in Ref. [18]. The corresponding values for A_{part} were obtained via the Glauber model [19]. Figures 2(a) and 2(b) show the respective centrality (A_{part}) dependence of the multiplicity for Ξ^- and ($\Lambda + \Sigma^0$) as the Λ yield includes feed-down contributions from the Σ^0. The ratio $\Xi^-/(\Lambda + \Sigma^0)$ is shown as a function of A_{part} in Fig. 2(c). Figures 2(a) and 2(b) indicate a relatively strong increase in the Ξ^- and ($\Lambda + \Sigma^0$) multiplicities with increasing A_{part}. However, this dependence is greater for the Ξ^- as can be seen in Fig. 2(c). An extrapolation (with the fit function multiplicity = const $\times$ A_{part}^{α}) to the data shown in Fig. 2(c) leads to the ratio $\Xi^-/(\Lambda + \Sigma^0)$ of 0.017 ± 0.005 for most central collisions ($b = 0$ fm or $A_{\text{part}} \sim 370$).

Figure 2 also shows the results of calculations from the transport model RQMD [17] as indicated. For the single-strange hyperons $\Lambda + \Sigma^0$, the model prediction of an increase in multiplicity with increasing centrality follows the trend of the data rather well. A similarly good agreement is apparent for the doubly strange Ξ^- hyperon. This rather striking agreement between data and theory is in direct contrast to the observation that transport models are unable to describe the measured yields for Ξ^- at SPS energies [11]. Next we compare the ratio $\Xi^-/(\Lambda + \Sigma^0)$ to that obtained at higher incident energies and to statistical-model predictions as shown in Fig. 3.

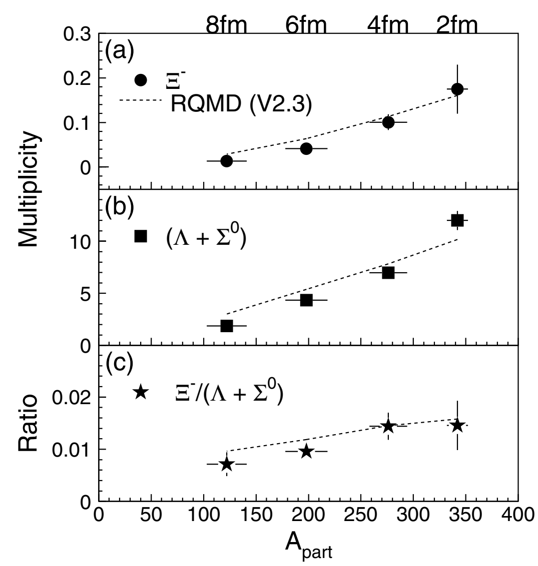

FIG. 2. (a),(b) A_{part} dependence of the multiplicity of Ξ^- (circles) and ($\Lambda + \Sigma^0$) (squares), respectively, from 6A GeV Au + Au collisions. Central collision have $A_{\text{part}} \sim 370$. (c) The corresponding multiplicity ratio (stars), $\Xi^-/(\Lambda + \Sigma^0)$, as a function of A_{part}. Values from RQMD calculations are indicated via the dotted lines.

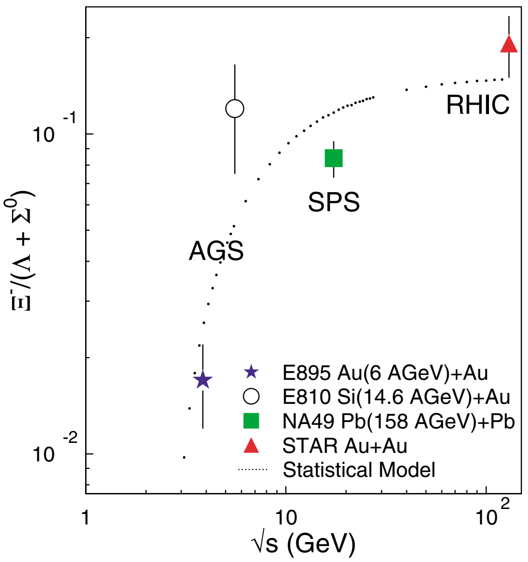

FIG. 3 (color online). The multiplicity ratio of $\Xi^-/(\Lambda + \Sigma^0)$ as a function of $\sqrt{(s)}$. Solid symbols correspond to central collisions of Au + Au/Pb + Pb. The datum indicated by the open circle is for the asymmetric system Si + Au. The dotted line shows results from the statistical model for central Au + Au collisions.

The statistical model makes predictions for this ratio as a function of $\sqrt{s}$ [20]. The general freeze-out curve [21] taken together with the values of the chemical freeze-out temperature T and baryochemical potential μ_B as a function of $\sqrt{s}$ [20] define all of the particle ratios. The dotted line in Fig. 3 indicates the ratio $\Xi^-/(\Lambda + \Sigma^0)$ calculated for central collisions. It exhibits a pronounced rise in the AGS/SPS energy regime and then flattens off toward the RHIC domain of $\sqrt{s} > 100$ GeV. Parameters for the statistical model are determined from the systematics of fits to experimental data, and hence have finite uncertainties. Therefore, the curve in Fig. 3 should in principle be replaced by a band. Evaluation of these uncertainties as a function of energy is beyond the scope of this work.

The rise up to SPS energies results from two primary effects. The first is an increase in temperature, from ≈ 50 MeV (SchwerIonenSynchrotron (heavy ion synchrotron), GSI) up to ≈ 170 MeV (SPS/RHIC). The second effect originates from the fact that one needs to use a canonical description at the lower incident energies. For central collisions at SPS energies, the number of multistrange particles is high and a grand-canonical description (global strangeness conservation) is sufficient. At lower incident energies, this number is much smaller, requiring a canonical treatment (local strangeness conservation) which leads to an additional suppression towards the lower incident energies [9]. Above top SPS energies the temperature is roughly constant, while μ_B decreases. Since the ratio $\Xi^-/(\Lambda + \Sigma^0)$ is independent of μ_B, it saturates (neglecting higher resonances which are taken into account in the model calculations) to the limit $g_{\Xi^-}/(g_\Lambda + g_{\Sigma^0}) \exp[-(E_{\Xi^-} + \mu_S - E_{\Lambda,\Sigma^0})/T]$, with g_i the degeneracy, μ_S the strangeness chemical potential, and E_i the energy of particle i. Detailed calculations for the centrality dependence are not yet available.

Data for Ξ^- production are indeed scarce. Results obtained at SPS from NA49 [22] and very recently at RHIC [23] for central collisions of Pb + Pb/Au + Au are shown as solid symbols in Fig. 3. The RHIC point (for midrapidity only) agrees (well) with the statistical model. The SPS point for the 4π integrated yield is below the statistical-model curve. At the highest AGS energy a data point (open circle) is shown for a Si + Au measurement performed at slightly forward rapidities ($y = 1.4$–2.9) [24]. This data point exceeds the curve, but is within 2 standard deviations even neglecting the systematic uncertainty in the statistical-model calculations. The solid star in Fig. 3 indicates our new 4π integrated result for central Au + Au collisions at $6A$ GeV. This value is in good agreement with the statistical-model prediction [20].

This data point is also in good agreement with the predictions of the RQMD model [cf. Fig. 2(c)]. Thus, we conjecture that hadronic processes are able to explain the measured yields. This is in agreement with recent ultrarelativistic quantum molecular dynamics calculations [25] which give a detailed account of the channels responsible for Ξ^- production. Since the statistical-model predictions also give a good representation of the data, the question is raised as to how far transport model calculations are from chemical equilibrium. Additional theoretical work is clearly needed to answer this question and to unravel the production mechanism(s) for multistrange hadrons from energies close to threshold up to the SPS (where current calculations fail to reproduce the measured yields by hadronic processes alone).

In conclusion, we have presented the first measurement for the doubly strange hyperon Ξ^- in near-threshold Au + Au collisions. The multiplicity of the Ξ^- is observed to increase more rapidly with centrality than the multiplicity of $\Lambda + \Sigma^0$, but the measured ratio $\Xi^-/(\Lambda + \Sigma^0)$ for central collisions agrees well with both statistical and transport model predictions. This agreement may be an indication that, despite the rather short reaction times at AGS energies, the available phase space for Ξ^- is essentially filled.

This work was supported in part by the U.S. Department of Energy under Grants No. DE-FG02-87ER40331, No. DE-FG02-89ER40531, No. DE-FG02-88ER40408, No. DE-FG02-87ER40324, and Contract No. DE-AC03-76SF00098; by the U.S. National Science Foundation under Grants No. PHY-98-04672, No. PHY-9722653, No. PHY-96-05207, No. PHY-9601271, and No. NT-9225096; by the University of Auckland Research Committee, NZ/U.S.A. Cooperative Science Programme CSP 95/33; and by the National Natural

Science Foundation of People's Republic of China under Grant No. 19875012.

[1] J. Rafelski, Phys. Lett. B **97**, 297 (1980); P. Koch, B. Müller, and J. Rafelski, Phys. Rep. **142**, 168 (1986).

[2] J. Rafelski, Phys. Lett. B **262**, 333 (1991).

[3] *Proceedings of the 6th International Conference on Strange Quarks in Matter, Frankfurt am Main, Germany, 2001* [J. Phys. G 28, 1517 (2002)].

[4] WA97 Collaboration, E. Andersen *et al.*, Phys. Lett. B **449**, 401 (1999); NA57 Collaboration, N. Carrer, *Quark Matter 2001, Stony Brook, New York, 2001* [Nucl. Phys. A698, 495c (2002)].

[5] P. Braun-Munzinger, J. Stachel, J. P. Wessels, and N. Xu, Phys. Lett. B **344**, 43 (1995); **365**, 1 (1996); P. Braun-Munzinger and J. Stachel, Nucl. Phys. **A606**, 320 (1996).

[6] P. Braun-Munzinger, I. Heppe, and J. Stachel, Phys. Lett. B **344**, 43 (1995).

[7] P. Braun-Munzinger, D. J. Magestro, K. Redlich, and J. Stachel, Phys. Lett. B **518**, 41 (2001).

[8] See, for example, *Quark Matter 2002, Nantes, France, 2002* [Nucl. Phys. A715, 761 (2003)].

[9] J. Cleymans, H. Oeschler, and K. Redlich, Phys. Rev. C **59**, 1663 (1999); Phys. Lett. B **485**, 27 (2001).

[10] J. S. Hamieh, K. Redlich, and A. Tounsi, Phys. Lett. B **486**, 61 (2000).

[11] S. Soff *et al.*, Phys. Lett. B **471**, 89 (1999).

[12] P. Chung *et al.*, J. Phys. G **25**, 255 (1999); C. Pinkenburg *et al.*, in *Proceedings of Quark Matter 2001, Stony Brook, New York, 2001* [Nucl. Phys. A698, 495c (2002)].

[13] G. Rai *et al.*, IEEE Trans. Nucl. Sci. **37**, 56 (1990).

[14] C. Pinkenburg *et al.*, Phys. Rev. Lett. **83**, 1295 (1999); P. Chung *et al.*, Phys. Rev. Lett. **85**, 940 (2000).

[15] M. Justice *et al.*, Phys. Lett. B **440**, 12 (1998).

[16] M. Justice, Nucl. Instrum. Methods Phys. Res., Sect. A **400**, 463 (1997).

[17] H. Sorge, Phys. Rev. C **52**, 3291 (1995).

[18] P. Chung *et al.*, Phys. Rev. C **66**, 021901(R) (2002).

[19] R. J. Glauber, Phys. Rev. **100**, 242 (1955).

[20] P. Braun-Munzinger, J. Cleymans, H. Oeschler, and K. Redlich, Nucl. Phys. **A697**, 902 (2002).

[21] J. Cleymans and K. Redlich, Phys. Rev. Lett. **81**, 5284, (1998); Phys. Rev. C **60**, 054908 (1999).

[22] Latest results with 4π yields are from NA49 Collaboration, S.V. Afanasiev *et al.*, Phys. Lett. B **538**, 275 (2002); NA49 Collaboration, A. Mischke *et al.*, in *Proceedings of the 6th International Conference on Strange Quarks in Matter, Frankfurt am Main, Germany, 2001* [J. Phys. G 28, 1761 (2002)].

[23] STAR Collaboration, J. Castillo *et al.*, in *Quark Matter 2002, Nantes, France, 2002* [Ref. [8]].

[24] E810 Collaboration, S. E. Eiseman *et al.*, Phys. Lett. B **325**, 322, (1994).

[25] M. Reiter *et al.*, in Proceedings of the Trento Workshop on Transport Model Calculations, Trento, Italy, 2003 (to be published).